Anomalies of water and hydrogen bond dynamics in hydrophobic nanoconfinement

Pradeep Kumar[1], Sungho Han[2] and H Eugene Stanley[2]

[1] Center for Studies in Physics and Biology, Rockefeller University, 1230 York Avenue, New York, NY 10021, USA
[2] Center for Polymer Studies and Department of Physics, Boston University, Boston, MA 02215, USA

Abstract

Using molecular dynamic (MD) simulations of the TIP5P model of water, we investigate the effect of hydrophobic confinement on the anomalies of liquid water. For confinement length $Lz = 1.1$ nm, such that there are 2–3 molecular layers of water, we find the presence of the bulk-like density and diffusion anomaly in the lateral directions. However, the lines of these anomalies in the P–T plane are shifted to lower temperatures ($\Delta T \approx 40$ K) and pressures compared to bulk water. Furthermore, we introduce a method to calculate the effective diffusion constant along the confinement direction and find that the diffusion anomaly is absent. Moreover, we investigate the hydrogen bond dynamics of confined water and find that the hydrogen bond dynamics preserves the characteristics of HB dynamics in bulk water, such as a non-exponential behavior followed by an exponential tail of HB lifetime probability distributions and an Arrhenius temperature dependence of the average HB lifetime. The average number and lifetime of HBs decrease in confined water compared to bulk water at the same temperature. This reduction may be the origin of the reasons for the different physical properties of confined water from bulk water, such as the 40 K temperature shift.

(Some figures in this article are in colour only in the electronic version)

1. Introduction

Water is the most ubiquitous liquid and hence plays a very important role in different phenomena. The list of such phenomena ranges across such varied disciplines as physics, chemistry, biology, nanofluidics, geology and atmospheric sciences [1–7]. Water also falls into a class of complex liquids which are known to have anomalous behavior compared to simple liquids [8, 9]. The anomalous expansion upon decreasing temperature below 4°C and increase of specific heat upon decreasing temperature in the supercooled state are some of the examples of the anomalies of water. Indeed, the list of the anomalous behaviors is incomplete and seems to be ever-growing [10, 11].

Water confined in nanoscale geometries has garnered much attention due to its biological and technological importance [12, 13]. Confinement can lead to changes in both structural and dynamical properties caused by the interaction with a surface [14–18]. Studies of water confined in carbon nanotubes and between hydrophobic surfaces suggest that the confining surfaces may induce layering in liquid water in extreme nanoconfinements [14, 15]. Moreover, first-order layering transitions are also observed [15, 19] in hydrophobic confinement. Apart from distinct structural changes, water also exhibits dynamic changes depending on the nature of the confining substrates. It has been found that the dynamics becomes slow near hydrophilic surfaces compared to hydrophobic surfaces, presumably due to the binding of polar oxygens and hydrogens to the polar groups on the hydrophilic substrates. Moreover, the dynamics in confinement may depend on the surface morphology. Specifically, it was found that a liquid in smooth confinements diffuses faster than when the confining surfaces are rough [20]. Slowing down of water dynamics near a hydrophilic surface has been experimentally observed [21]. Water confined in Vycor [22, 23] has at least two different dynamical regimes arising from the slow dynamics of water near the surface and the fast dynamics of water far away from the surfaces [24–29].
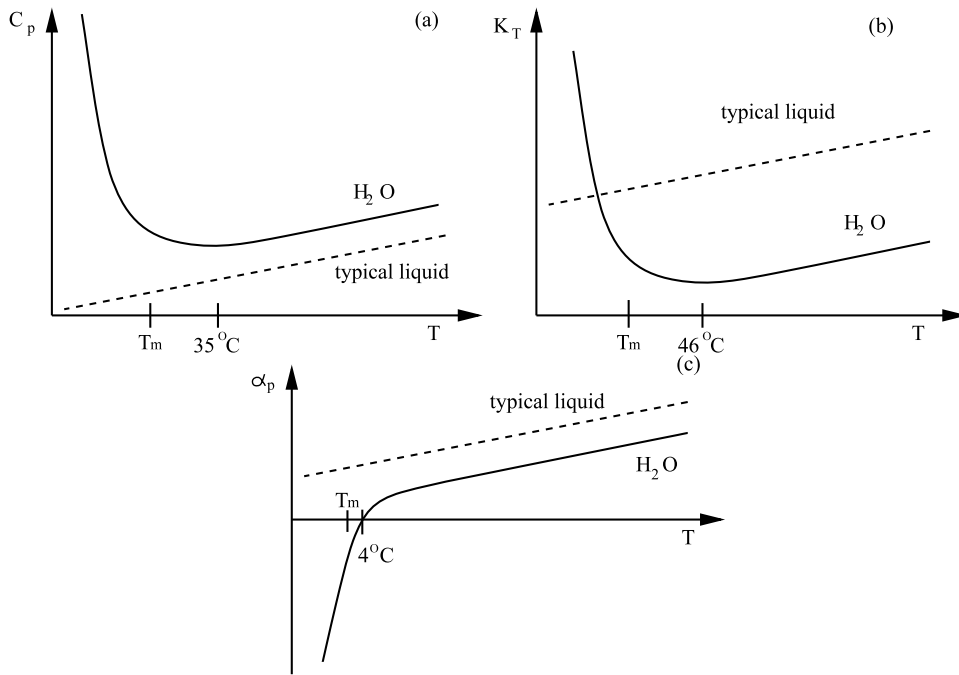
Figure 1. Schematic representation of response functions: (a) C_P, (b) k_T and (c) α_P of liquid water as a function of temperature T. The behavior of a normal liquid is shown as dashed curves.

Recent studies [16, 30–33] suggest that both thermodynamic and dynamic anomalies of water are strongly affected when water is confined in small nanopores. It is found that, when water is confined between hydrophobic surfaces, both thermodynamic and dynamic anomalies shift to low temperatures and low pressures compared to bulk water [16, 30]. Although the characteristics of hydrogen bond dynamics of water is bulk-like in hydrophobic confinement, the average lifetime decreases [34] leading to a shift in the regions of anomalous dynamics and thermodynamics in the P–T plane [16, 30, 31, 33]. Moreover, the long time relaxation of hydrogen bonds depends on the effective system dimensionality.

In this paper, we study the effect of smooth hydrophobic confinement on the anomalies and hydrogen bond dynamics of water using molecular dynamics simulations of the TIP5P [35] model of water.

2. Thermodynamic and dynamic anomalies of bulk water

What makes water more interesting compared to many other liquids are the properties of water, also called the *anomalies of water*. Due to its very puzzling nature, water has been the subject of intense studies for decades. One, regarding the well-known anomaly of the density maximum at 4 °C [36], dates backs to the seventeenth century. In the supercooled region most of the anomalous properties of water get more enhanced [37].

2.1. Density anomaly

The density anomaly is perhaps one of the oldest known puzzling behaviors of water. Unlike other simple liquids which

expand upon heating, water expands upon cooling below 277 K at ambient pressure. It is due to this anomaly that ice floats on water and fish can survive in warm waters below a layer of ice at temperatures well below 0 °C. The temperature of maximum density T_{MD} moves to lower temperatures as the pressure is increased and disappears above ≈200 MPa. The locus of T_{MD} carves out a wide region in the (T, P) plane, where the density anomaly occurs.

2.2. Specific heat

A schematic of isobaric heat capacity C_P for liquid water at atmospheric pressure is shown in 1(a). C_P is a measure of entropy fluctuations and is related to entropy fluctuations [38, 39] as

$$C_P = \left(\frac{dH}{dT} \right)_P = T \left(\frac{\partial S}{\partial T} \right)_P = \frac{\langle (\Delta S)^2 \rangle}{k_B}. \qquad (1)$$

Since any thermal fluctuation should decrease with decreasing temperature, one would expect that C_P should decrease upon decreasing temperature: however, for the case of water it increases sharply as the temperature is decreased below ≈330 K and seems to diverge at a singular temperature with a power law [40].

2.3. Isothermal compressibility

A schematic of isothermal compressibility k_T for water is shown in figure 1(b). Like C_P, k_T is the measure of volume fluctuations:

$$k_T = -\frac{1}{V} \left(\frac{\partial V}{\partial P} \right)_T = \frac{(\Delta V)^2}{k_B T V}. \qquad (2)$$
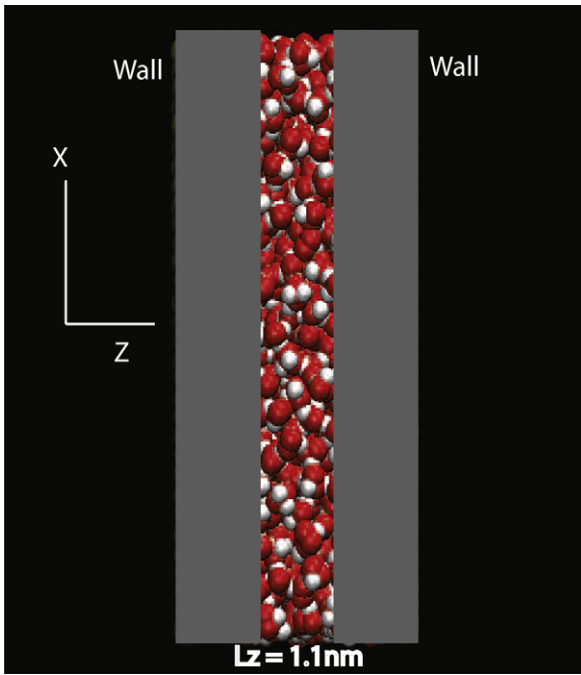
Figure 2. Schematic of liquid water confined between two surfaces separated by 1.1 nm. The effective width due to excluded-volume interaction between the water molecules and the surfaces is 0.8 nm, which can hold two to three molecular layers of water, depending on the density.

Intuitively k_T should decrease upon decreasing the temperature. In the case of water, instead, it increases like C_P and seems to diverge with a power law at a lower temperature in experiments [40].

2.4. Coefficient of thermal expansion

The coefficient of thermal expansion, α_P, is the measure of cross fluctuations of volume and entropy:

$$\alpha_P = -\frac{1}{V}\left(\frac{\partial V}{\partial T}\right)_P = \frac{P}{k_B{}^2 T}\langle \Delta V \Delta S\rangle, \qquad (3)$$

Figure 1(c) shows the behavior of α_P. α_P is positive for normal liquids. However, in the case of water it becomes negative at the temperature of maximum density T_{MD} at constant pressure, suggesting that below this as the volume is increased the entropy decreases. Like other response functions, α_P also seems to diverge with a power law at low temperatures in experiments. Dashed curves in figure 1 are the schematic representations of the behavior of normal liquids for comparison.

Since the experiments on bulk liquid water cannot be performed below the homogeneous nucleation temperature $T_H \approx -38°$, where the crystal formation is inevitable, it is not possible to test for bulk water whether the seeming divergence of response functions at low temperatures is indeed a divergence or something else. Recent experimental [41–43] and computational studies [44] find that the response functions do not diverge but have a maximum at low temperatures.

2.5. Diffusion anomaly

The dynamics of simple liquids becomes slower upon pressurizing: however, the dynamics of water becomes faster as the pressure is increased, reaching a maximum at a constant temperature. The region of this dynamic anomaly is wider than the density anomaly region in the (T, P) plane. The anomalous increase of diffusion upon pressurizing is attributed to the breaking of hydrogen bonds. As the pressure is increased more and more hydrogen bonds are broken, making the water molecules diffuse free from their neighbors and hence the increase of diffusion.

2.6. Dynamic crossover at low temperatures

Recent experiments on water confined in nanoscale pores [41] and hydration water [42] around biomolecules find that the behavior of the dynamics of water changes from 'non-Arrhenius' at high temperatures, where the activation energy changes with temperature, to 'Arrhenius' at low temperatures, where the activation energy varies little with temperature. This behavior of the dynamics of liquid water is in contrast to the presumed behavior of the dynamics (such as viscosity or diffusion constant) which would follow a non-Arrhenius behavior as a function of temperature all the way down to the glass transition.

3. Thermodynamic and dynamic anomaly of liquid water in smooth hydrophobic confinement

We perform molecular dynamics (MD) simulations of a system composed of $N = 512$ water-like molecules confined between two smooth walls. The molecules interact via the TIP5P pair potential [35] which, like the ST2 [45] potential, treats each water molecule as a tetrahedral, rigid and non-polarizable unit consisting of five point sites. Two positive point charges of charge $q_H = 0.241e$ (where e is the fundamental unit of charge) are located on each hydrogen atom at a distance 0.095 72 nm from the oxygen atom; together they form an HOH angle of 104.52°. Two negative point charges ($q_e = -q_H$) representing the lone pair of electrons (e^-) are located at a distance 0.07 nm from the oxygen atom. These negative point charges are located in a plane perpendicular to the HOH plane and form an e^-Oe^- angle of $\cos^{-1}(1/3) = 109.47°$, the tetrahedral angle. To prevent the overlap of molecules, a fifth interaction site is located on the oxygen atom, and is represented by a Lennard-Jones (LJ) potential with parameters $\sigma_{oo} = 0.312$ nm and $\epsilon_{oo} = 0.6694$ kJ mol^{-1}.

The TIP5P potential accurately reproduces many water anomalies when, for example, its structural properties compare well with experiments [35, 46–48]. TIP4P and TIP5P are known to crystallize [46, 49] within accessible computer simulation timescales, showing a 'nose-shaped' curve of temperature versus crystallization time, a feature found in experimental data on water solutions [50]. TIP5P simulations also show a van der Waals loop in the P–ρ plane at the lowest T accessible with current computation facilities [46]. This loop indicates the presence of a first-order LL transition. Reference [46] estimates that an LL transition line ends in
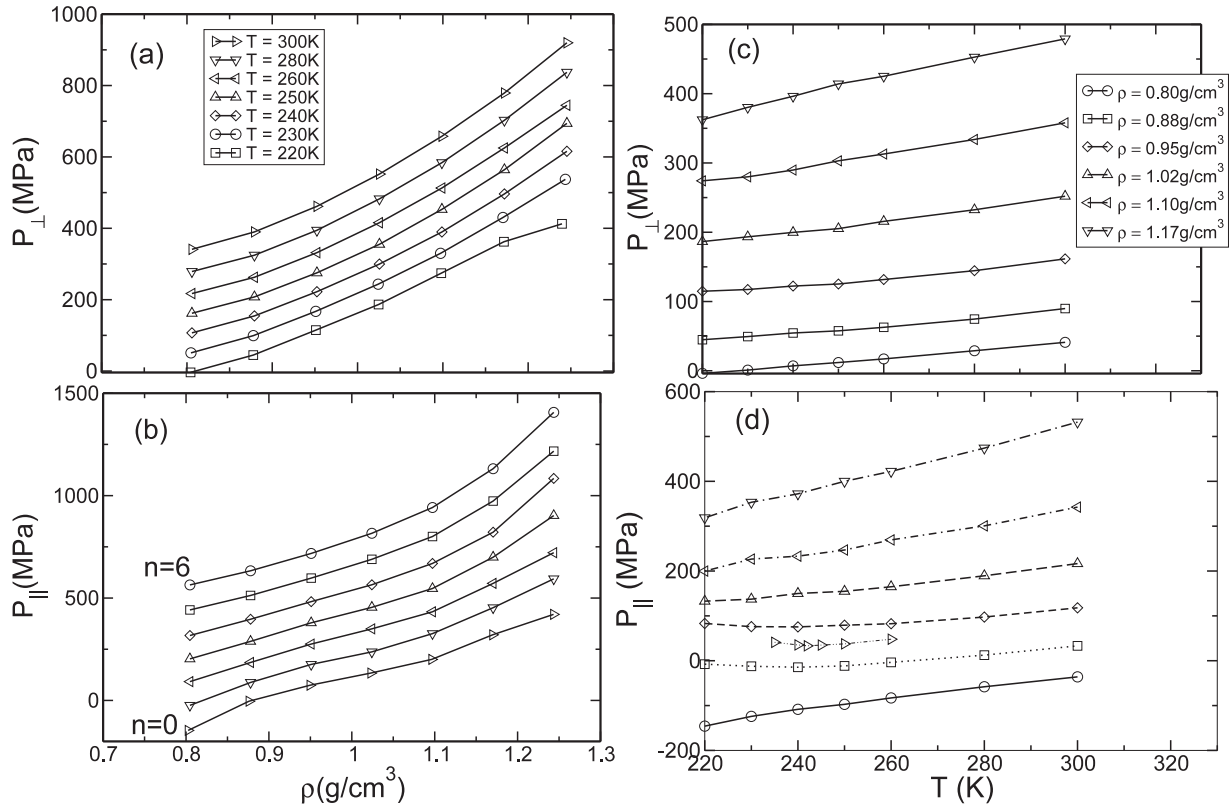
Figure 3. (a) Transverse pressure $P_\perp$ (perpendicular to the walls) and (b) lateral pressure $P_\parallel$ (parallel to the walls) as functions of density ρ for all simulated T. For clarity, each curve is shifted by $n \times 50$ MPa for $P_\perp$ and $n \times 100$ MPa for $P_\parallel$. While $P_\perp$ shows no inflection for all T, $P_\parallel$ starts to flatten at $\rho \approx 0.87$ g cm^{-3} for the lowest T presented. This is consistent with the possibility of a second critical point at lower than $T = 220$ K. (c) Transverse pressure $P_\perp$ as a function of T. (d) Lateral pressure $P_\parallel$ as a function of temperature T for different densities.

an LL critical point C′ located at $T_{C'} = 217 \pm 3$ K, $P_{C'} = 340 \pm 20$ MPa and $\rho_{C'} = 1.13 \pm 0.04$ g cm^{-3}.

In our simulation, water molecules are confined between two infinite smooth planar walls, as shown schematically in figure 2. The walls are located at $z = \pm 0.55$ nm, corresponding to a wall–wall separation of 1.1 nm, which results in $\approx$2–3 layers of water molecules. Periodic boundary conditions are used in the x and y directions, parallel to the walls.

The interactions between water molecules and the smooth walls are designed to mimic solid paraffin [51] and are given by [52]

$$U(\Delta z) = 4\epsilon_{ow}\left[\left(\frac{\sigma_{ow}}{\Delta z}\right)^9 - \left(\frac{\sigma_{ow}}{\Delta z}\right)^3\right]. \quad (4)$$

Here Δz is the distance from the oxygen atom of a water molecule to the wall, while $\epsilon_{ow} = 1.25$ kJ mol^{-1} and $\sigma_{ow} = 0.25$ nm are potential parameters. The same parameter values were used in previous confined water simulations [51, 53].

We perform simulations for 56 state points, corresponding to seven temperatures $T = 220, 230, 240, 250, 260, 280$ and 300 K, and eight densities $\rho = 0.80, 0.88, 0.95, 1.02, 1.10, 1.17, 1.25$ and 1.32 g cm^{-3}.[3] The range of density values takes

---

[3] We note that the accessible volume to the water molecules is not given by the total geometrical volume between the walls, $V = L_x L_y L_z$. Instead, the accessible volume is given by $V' = L_x L_y L_z'$, where $L_z' < L_z$ due to the repulsive wall–water interactions for short distances.

into account the fact that the water–wall interactions prevent water molecules from accessing a space near the walls. Our determination of ρ is discussed in detail in section 4. The raw 'geometric' densities used are $\rho = 0.60, 0.655, 0.709, 0.764, 0.818, 0.873, 0.927$ and 0.981 g cm^{-3}.

For each state point, we perform two independent simulations to improve the statistics. We control the temperature using the Berendsen thermostat with a time constant of 5 ps [54] and use a simulation time step of 1 fs, just as in the bulk system [46]. For long-range interactions we use a cutoff of 0.9 nm [35].

Unlike bulk liquid systems, one must be careful to interpret separately the results involving the lateral pressure $P_\parallel$ and those involving the transverse pressure $P_\perp$, since the thermodynamic averages of these quantities will usually be different. Phase separation will only be apparent in $P_\parallel$, since the separation of the plates is too small to allow for the existence of two distinct phases in the transverse direction. In figures 3(a) and (b), we show $P_\perp$ and the lateral pressure $P_\parallel$ as functions of density along all seven isotherms. Figures 3(c) and (d) show the T dependence of $P_\perp$ and $P_\parallel$ for different densities. $P_\perp(\rho)$ is a monotonic function of ρ. Similar behavior is observed for $P_\parallel(\rho)$ at high T. However, for 0.88 g cm$^{-3} \leqslant \rho \leqslant 1.17$ g cm^{-3}, the isochores in the $P_\parallel$–ρ plane display minima, indicating the presence of a T_{MD} line defined as the locus of points where $(\partial P / \partial T)_V = 0$ [52]. For $T < T_{MD}$, water confined between hydrophobic walls is

anomalous, i.e. it becomes less dense upon cooling. A T_{MD} line has also been found in TIP5P bulk water simulations [46]. Comparison of figure 3(c) and figure 2(a) of [46] shows that the T_{MD} locus in confined water shifts to lower T. We also plot the T_{MD} for bulk water (from [46]) and confined water in figure 4. A +40 K temperature shift in the T_{MD} of confined water overlaps these loci. Thus the effect of the hydrophobic walls in our system seems to be to shift the P–T phase diagram by $\Delta T \approx -40 \pm 5$ K with respect to bulk water. This is consistent with the second critical point shifting to lower T. Thus far, we have seen that the density anomaly shifts to lower temperatures in smooth confinement considered here. Hence it is natural to consider whether the dynamic properties of confined water exhibit the same temperature shift found for the thermodynamic properties relative to bulk water. For example, how is the maximum in diffusivity under pressure shifted under confinement? To compare with the bulk system, we calculate the lateral mean square displacement (MSD). We can evaluate the diffusion coefficient D from the asymptotic behavior of the lateral MSD using the Einstein relation

$$\langle r_\parallel^2 \rangle = 2dDt, \tag{5}$$

where $\langle r_\parallel^2 \rangle$ is the mean square displacement parallel to the walls over a given time interval t and d is the system dimension [52]. Since we calculate the diffusion only in the lateral directions, $d = 2$.

Figures 5(a) and (b) show the dependence of the lateral MSD on ρ at fixed $T = 230$ and 300 K. We also plot the dependence of the lateral MSD on T for two different temperatures in figures 5(c) and (d), using a log–log scale to emphasize the different mechanisms seen on different timescales, all of which are qualitatively similar to that of bulk water.

(i) An initial ballistic motion, where the lateral MSD is a quadratic function of time, $\langle r_\parallel^2(t) \rangle \sim t^2$.
(ii) An intermediate 'flattening' of the lateral MSD, due to the transient caging of molecules by their hydrogen bonded neighbors. This effect is most noticeable at the lowest T studied and does not occur at high T.
(iii) Long timescales on which particles diffuse randomly, and so $\langle r_\parallel^2(t) \rangle \sim t$.

　　To determine whether there is an anomaly in the density dependence of D, we plot D along isotherms, in figure 6(a) for confined water and in figure 6(b) for bulk water. For $T \lesssim 250$ K, we find that D has a maximum at $\rho \approx 1.05$ g cm^{-3}. In bulk water, a similar behavior is found, but at $T \approx 290$ K, 40 K higher than the confined system. Moreover, this shift in a dynamic anomaly is consistent with the shift of thermodynamic anomalies. Qualitatively, the maximum in D can be understood as a competition between weakening or breaking of hydrogen bonds under pressure [55] (which increases D) and increased packing (which reduces D).

4. Absence of diffusion anomaly in confinement direction

In [32] Han *et al* studied the diffusion along the confinement direction. To calculate the effective diffusion constant we
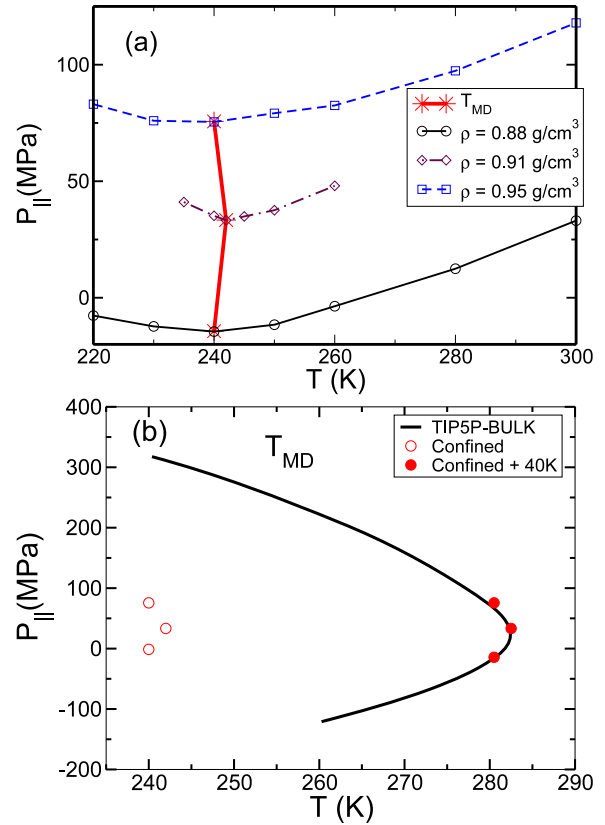

Figure 4. A comparison of T_{MD} line for bulk and confined water. (a) Isochores corresponding to the densities $\rho = 0.88, 0.91$ and 0.95 g cm^{-3} which have a minimum. The locus of the points where $(\partial P_\parallel / \partial T)_V = 0$ denotes the T_{MD} (shown as an asterisk). (b) If the T_{MD} for confined water (open circles) were shifted by 40 K, it would overlap the T_{MD} for bulk water (filled circles).

divide the system into three residence regions along the z direction such that there are two symmetric adjacent regions to the surface and one middle region. The width of each region is 0.14 nm and the separation between two adjacent regions is $Rz = 0.28$ nm, which is the same as the linear size of a water molecule. Then, we calculate the residence time distributions $P(\tau_R)$ of water molecules in the given residence region. The residence time is defined as the time over which water molecules stay in one region before leaving it. We find that $P(\tau_R)$ of the hydrophobic confined water decays exponentially for all temperatures investigated [32]. It was shown that the anomalous dynamics of water becomes subdiffusive when it is confined in Vycor pores with the condition of low hydration [56]. This subdiffusive motion is related to a power-law behavior of $P(\tau_R)$. However, our results show that, in hydrophobic confinement, $P(\tau_R)$ has an exponential behavior for all densities investigated. We calculate the characteristic residence time τ_R^C by finding the inverse slope of a straight line fit to $P(\tau_R)$ on the semilog plot:

$$P(\tau_R) \sim \exp\left(-\frac{\tau_R}{\tau_R^C}\right). \tag{6}$$

On average, during τ_R^C water molecules diffuse the same distance as the separation of two defined regions. Since water
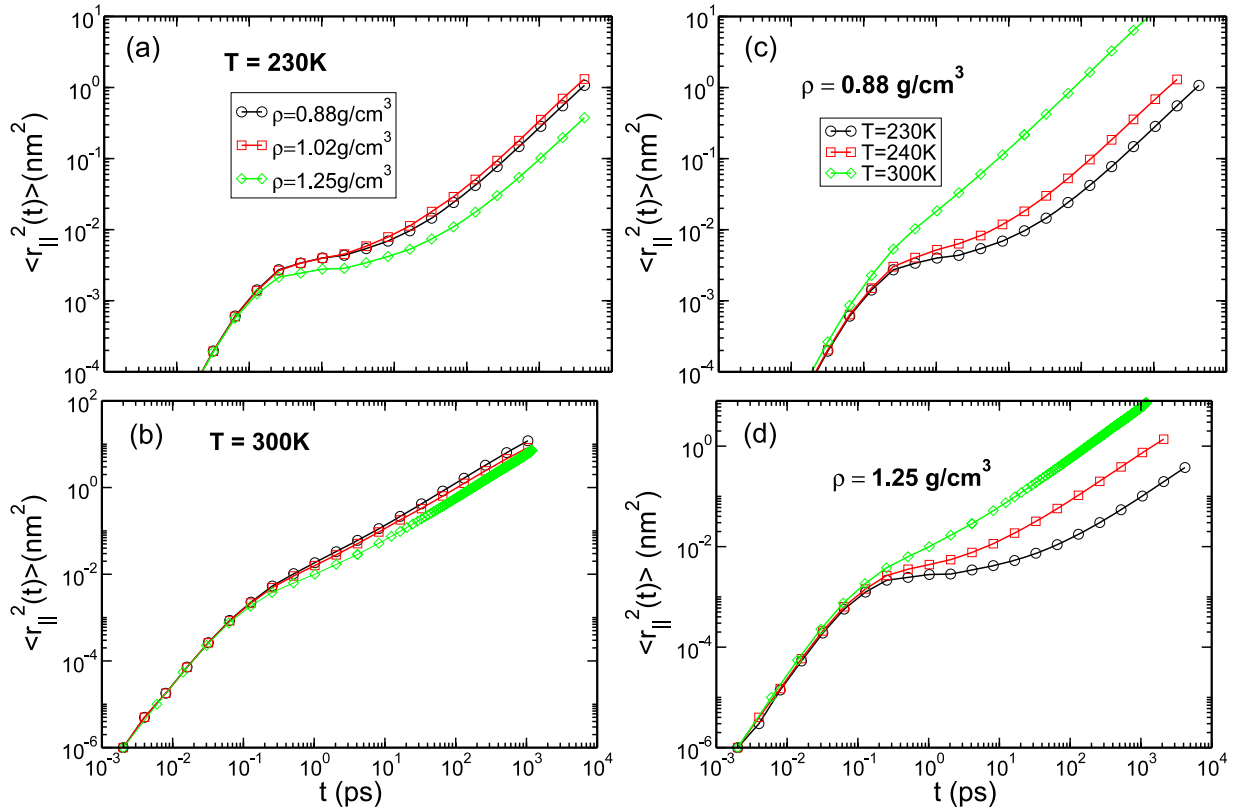
Figure 5. Lateral mean square displacement for different densities at constant temperatures (a) $T = 230$ K and (b) $T = 300$ K. Also shown are the MSD for different temperatures at constant densities (c) $\rho = 0.88$ g cm^{-3} and (d) $\rho = 1.25$ g cm^{-3}.

molecules diffuse a distance equal to the separation between two regions, on average, during the time interval τ_C, we can write down the diffusion coefficient $D_\perp$:

$$D_\perp = \frac{\langle R_z^2 \rangle}{2 \langle \tau_R^C \rangle} \qquad (7)$$

where $D_\perp$ is the diffusion coefficient in the direction perpendicular to the walls, $\langle R_z \rangle$ denotes the separation between two residence regions and $\langle \tau_R^C \rangle$ is the characteristic residence time averaged over an ensemble. To get the average value of $D_\perp$, we use the characteristic residence times averaged over three different residence regions. We find that $P(\tau_R)$ has the same exponentially decaying behavior in different residence regions for all temperatures investigated [32].

In figure 7, we show $D_\perp$ as a function of density for all temperatures studied. $D_\perp$ decreases as the density increases. Contrary to the diffusion anomaly found in the parallel direction (similar to bulk water), our results show a diffusion anomaly in the perpendicular direction does not exist down to the lowest temperature we simulated. As a result, we come to conclude that, by the nanoconfinement, a diffusion anomaly of water is absent in the confining direction at low temperatures. From the fact that a diffusion anomaly exists in the parallel direction but not in the perpendicular direction, the main contribution to the absence of a diffusion anomaly in the perpendicular direction might be the nanoconfinement itself rather than the hydrophobicity of the confining walls.

5. Hydrogen bond dynamics in smooth hydrophobic confinement

Previous hydrogen bond (HB) studies in confined systems showed that, compared to bulk water, the HB relaxation time, τ_R, in water confined in micelles [57, 58], as well as at vapor–water and metal–water interfaces [59], is longer. For water confined to the interior of carbon nanotubes, the HB lifetime becomes longer [60] or shorter [61] than that in bulk water, depending on the conditions in the system. In [34], Han *et al* studied the HB dynamics of water confined in a quasi-two-dimensional hydrophobic nanopore slit. Han *et al* performed MD simulations for a fixed water density $\rho = 1.02$ g cm^{-3} and for eight temperatures from 300 down to 230 K for the confined system studied above.

To investigate the HB dynamics, we use the geometric definition of HB, which is that two tagged molecules are considered to be bonded if simultaneously their inter-oxygen distance is less than 3.5 Å and the angle between intra-O–H and inter-O$\cdots$O is less than 30° [55, 62]. We calculate the probability density function (PDF) $P(t)$ of the HB lifetimes in both confined and bulk water (figure 8). We find that $P(t)$ in confined water decays slightly faster than in bulk water at the same temperature. The non-exponential behavior followed by an exponential tail of $P(t)$ is preserved as in the case of bulk water. However, we find that $P(t)$ of bulk water overlaps $P(t)$ for confined water when the bulk temperature is $\sim$40 K higher than the confined temperature. This shift in the PDF of lifetime
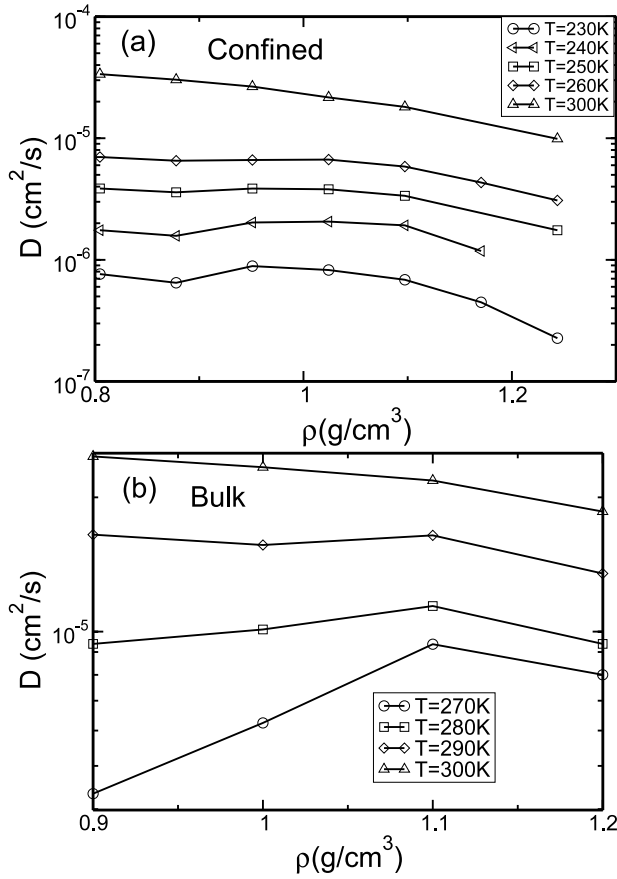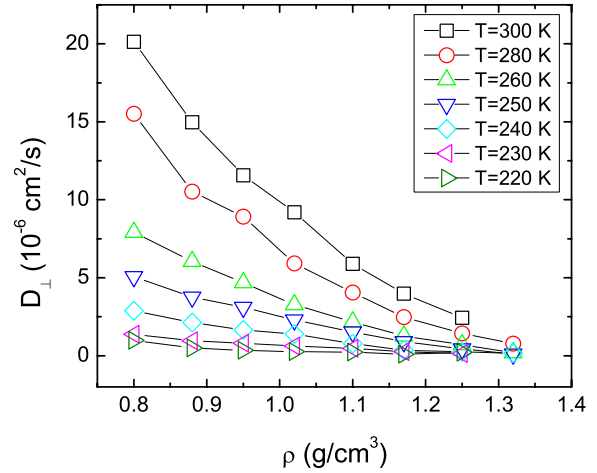
Figure 7. The diffusion coefficients in the perpendicular direction as a function of the density along the isotherms. At low temperature, the diffusion coefficients decrease with the increase of the density. It shows there is no diffusion anomaly along the perpendicular direction. In the parallel direction, there is a diffusion anomaly at temperatures lower than $T = 250$ K. (See [16].)
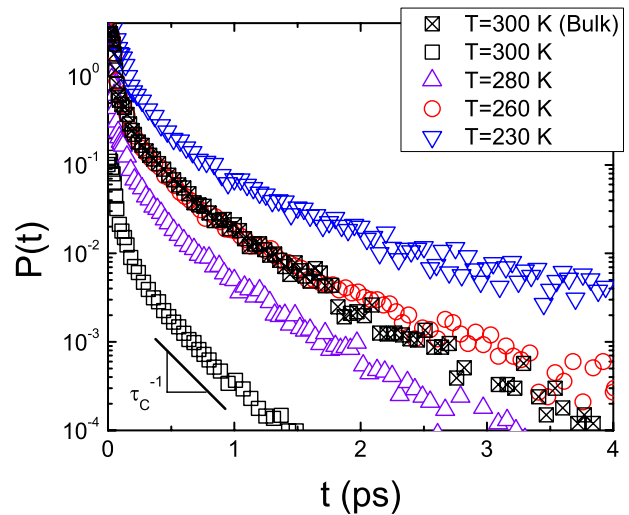

Figure 6. Diffusion constant as a function of density for various temperatures in (a) confined water and (b) bulk water. Confined water shows diffusion anomalies at lower temperatures than in bulk water. The first diffusion anomaly (the increase of diffusion with increase in density) in the confined system begins to appear when the temperature drops to $T \approx 250$ K, which is ≈ 40 K lower than in bulk water (which displays diffusion anomalies at $T \approx 290$ K).

Figure 8. Shown in a semilog plot are the distributions $P(t)$ of hydrogen bond lifetimes t at different temperatures. The plots, except $T = 300$ K for confined water, are shifted up for clarity. $P(t)$ indicates that there is a region which shows a non-exponential behavior, followed by an exponential tail for all temperatures investigated. Note that $P(t)$ for $T = 260$ K for confined water and $T = 300$ K for bulk water overlap, corresponding to the 40 K shift proposed for hydrophobic confinement. The line segment has slope τ_C^{-1}, since $P(t) \sim \exp(-t/\tau_C)$ in long timescales.

may be the origin of reasons for the shift of temperature ($\Delta T \sim 40$ K), at which anomalous thermodynamic behaviors appear, found in our simulations of hydrophobically confined water [16, 24] and also temperature shift ($\Delta T \sim 35$ K) of dynamic crossover experimentally found for water confined in carbon nanotubes [63]. Since $P(t)$ has an exponential tail, one can calculate the characteristic time τ_C defined by $P(t) \sim \exp(-t/\tau_C)$ at long timescales. We find that the temperature dependence of τ_C can be fitted by an Arrhenius form [34].

In figure 9, we calculate in both confined and bulk water the average HB lifetimes

$$\tau_{HB} \equiv \int_0^{\infty} t P(t) \, dt. \qquad (8)$$

We define τ_{HB} as the *continuous* HB lifetime [64], which means that HB remains intact during this time. Generally, τ_{HB} represents *fast* motion of HB related to the librational motion [55]. In figure 9, we show τ_{HB} as a function of temperature for both bulk and confined water. We find the temperature dependence of τ_{HB} is Arrhenius, described by $\tau_{HB} = \tau_0 \exp(E_A/k_B T)$. Notice that τ_{HB} for both

bulk and confined water has an Arrhenius dependence on temperature, but with different activation energy E_A, which has been interpreted as the energy required to break an HB via librational motion [55]. Further, we find that the activation energy E_A of confined water ($E_A^C = 4.92 \pm 0.07$ kJ mol^{-1}) is about half that in bulk water ($E_A^B = 9.80 \pm 0.53$ kJ mol^{-1}).[4] As

[4] This activation energy for bulk water is consistent with the activation energy $E_A = 10.8 \pm 1.0$ kJ mol^{-1} obtained from depolarized light scattering experiments [65].
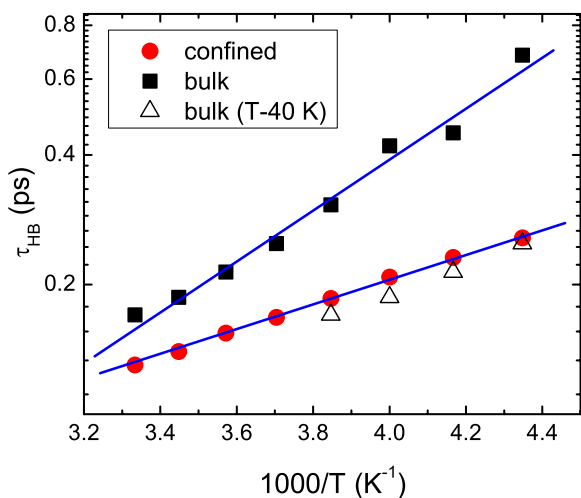
Figure 9. The average HB lifetime, τ_{HB}, as a function of $1/T$ in an Arrhenius plot. Two blue lines indicate the fits, $\tau_{HB} = \tau_0 \exp(E_A/k_B T)$. For confined water, τ_{HB} can be fitted by an Arrhenius behavior, which is preserved as in bulk water, even if τ_{HB} and the number of hydrogen bonds in confined water is smaller than in bulk water. The magnitude of activation energy calculated for confined water ($E_A^C = 4.92 \pm 0.07$ kJ mol^{-1}) is around half of that in bulk water ($E_A^B = 9.80 \pm 0.53$ kJ mol^{-1}). E_A^B is consistent with previous experimental and simulation results for the activation energy associated with fast hydrogen bond dynamics. The triangle symbols are for bulk water at temperatures shifted lower by $\Delta T = 40$ K.

a result, τ_{HB} in confined water is smaller than in bulk water at the same temperature. As for the PDF of HB lifetime, $\tau_{HB}(T)$ in bulk water can be matched to $\tau_{HB}(T)$ in confined water by shifting to lower temperature by 40 K, suggesting that the origin of the temperature shift in thermodynamic properties in confined water may be due to the change in the HB lifetime. However, $\langle n_{HB} \rangle$ in bulk water is *not* the same as that in confined water when temperature is shifted downward by $\approx$40 K [32].

6. Summary and discussions

Our results indicate that the region of density anomaly (whereby the density of water increases upon increasing temperature) and the region of diffusion anomaly (whereby the diffusion coefficient increases on increasing pressure) are shifted to lower temperatures and densities in the phase diagram relative to bulk water. Hence, the confined water can be said to have a higher 'effective' temperature, by $\approx$40 K, and higher 'effective' density $\approx$0.30 g cm^{-3}, relative to the bulk water. Additionally the liquid–liquid phase transition found for bulk water using the same model of water (TIP5P) is inaccessible in the temperature range where we may perform equilibrium simulations. Furthermore, we introduce a method to calculate the effective diffusion constant along the confinement direction and find that, although the diffusion anomaly in present in the lateral direction, it is absent in the direction along the confinement. Moreover, we find that confined water preserves the characteristics of HB dynamics in bulk water, such as a non-exponential behavior followed by an exponential tail of HB lifetime probability distributions and an

Arrhenius temperature dependence of the average HB lifetime. The average number and lifetime of HBs decrease in confined water compared to bulk water at the same temperature. This reduction may be the origin of the reasons for the different physical properties of confined water from bulk water, such as the 40 K temperature shift.

References

[1] Bellissent-Funel M-C (ed) 1999 *Hydration Processes in Biology: Theoretical and Experimental Approaches* (*Proc. NATO Advanced Study Institutes* vol 305) (Amsterdam: IOS Press)
[2] Ball P 2008 *Chem. Rev.* **108** 74
[3] Kumar P, Yan Z, Xu L, Mazza M G, Buldyrev S V, Chen S-H, Sastry S and Stanley H E 2006 *Phys. Rev. Lett.* **97** 177802
[4] Buldyrev S V, Kumar P, Debenedetti P G, Rossky P and Stanley H E 2007 *Proc. Natl Acad. Sci. USA* **104** 20177
[5] Michaelides A and Morgenstern K 2007 *Nat. Mater.* **6** 597
[6] Carrasco J, Michaelides A, Forster M, Haq S, Raval R and Hodgson A 2009 *Nat. Mater.* **8** 427
[7] Rasaiah J C, Garde S and Hummer G 2008 *Annu. Rev. Phys. Chem.* **59** 713
[8] Frank F (ed) 1972 *Water: A Comprehensive Treatise* (*The Physics and Physical Chemistry of Water vol 1*) (New York: Plenum)
[9] Debenedetti P G and Stanley H E 2003 *Phys. Today* **56** (6) 40
[10] Stanley H E *et al* 2007 *Physica* A **386** 729
[11] http://www.lsbu.ac.uk/water/
[12] Zangi R 2004 *J. Phys.: Condens. Matter* **16** S5371
[13] Gelb I D, Gubins K E, Radhakrishnan R and Bartkoviak M S 1999 *Rep. Prog. Phys.* **61** 1573
[14] Koga K 2003 *J. Chem. Phys.* **118** 7973
[15] Zangi R 2004 *J. Phys.: Condens. Matter* **16** S5371
[16] Kumar P, Buldyrev S V, Starr F W and Stanley H E 2005 *Phys. Rev.* E **72** 051503
[17] Giovambattista N, Rossky P J and Debenedetti P G 2009 *Phys. Rev. Lett.* **102** 050603
[18] Giovambattista N, Debenedetti P G and Rossky P J 2007 *J. Phys. Chem.* C **111** 1323
[19] Koga K, Tanaka H and Zeng X C 2000 *Nature* **408** 564
[20] Scheidler P, Kob W and Binder K 2002 *Europhys. Lett.* **59** 701
[21] Bellissent-Funel M-C, Sridi-Dorbez R and Bosio L 1996 *J. Chem. Phys.* **104** 10023
[22] Chen S-H, Gallo P and Bellissent-Funel M-C 1995 *Can. J. Phys.* **73** 703
[23] Chen S-H and Bellissent-Funel M-C 1994 *Hydrogen Bond Networks* (*NATO ASI Ser. C: Math. Phys. Sci.* vol 435) ed M-C Bellissent-Funel and J C Dore (Dordrecht: Kluwer Academic) p 337
[24] Gallo P and Rovere M 2002 *J. Phys.: Condens. Matter* **15** 1521
[25] Spohr E, Hartnig C, Gallo P and Rovere M 1999 *J. Mol. Liq.* **80** 165
[26] Gallo P, Ricci M A, Rovere M, Hartnig C and Spohr E 2000 *Europhys. Lett.* **49** 183
[27] Hartnig C, Witschel W, Spohr E, Gallo P, Ricci M A and Rovere M 2000 *J. Mol. Liq.* **85** 127
[28] Gallo P, Rovere M, Ricci M A, Hartnig C and Spohr E 1999 *Phil. Mag.* B **79** 1923
[29] Gallo P 2000 *Phys. Chem. Chem. Phys.* **2** 1607
[30] Corradini D, Gallo P and Rovere M 2008 *J. Chem. Phys.* **128** 244508
[31] Brovchenko I and Oleinikova A 2007 *J. Chem. Phys.* **126** 214701
[32] Han S, Kumar P and Stanley H E 2008 *Phys. Rev.* E **77** 030201(R)
[33] Truskett T M and Debenedetti P G 2001 *J. Chem. Phys.* **114** 2401

[34] Han S, Kumar P and Stanley H E 2009 *Phys. Rev.* E **79** 041202
[35] Mahoney M W and Jorgensen W L 2000 *J. Chem. Phys.*
112 8190
[36] Röntgen W C 1892 Ueber die constitution des flüssigen
wassers *Ann. Phys. Chem.* **45** 91–7
[37] Debenedetti P G 2003 *J. Phys.: Condens. Matter* **15** R1669
[38] Stanley H E 1971 *Introduction to Phase Transitions and
Critical Phenomena* (London: Oxford Scince Publication)
[39] Huang K 2001 *Introduction to Statistical Physics* (London:
Francis and Taylor)
[40] Angell C A 1995 Formation of glasses from liquids and
biopolymers *Science* **267** 1924–35
[41] Liu L, Chen S-H, Faraone A, Yen C-W and Mou C Y 2005
Phys. Rev. Lett. **95** 117802
[42] Chen S-H *et al* 2006 *Proc. Natl Acad. Sci. USA* **103** 9012
[43] Mallamace F, Branca C, Broccio M, Corsaro C, Mou C-Y and
Chen S-H 2007 *Proc. Natl Acad. Sci. USA* **104** 18387–91
[44] Xu L *et al* 2005 *Proc. Natl Acad. Sci. USA* **102** 16558
[45] Stillinger F H and Rahman A 1974 *J. Chem. Phys.* **60** 1545
[46] Yamada M *et al* 2002 *Phys. Rev. Lett.* **88** 195701
[47] Mahoney M W and Jorgensen W L 2001 *J. Chem. Phys.*
114 363
[48] Sorenson J M, Hura G, Glaeser R M and Head-Gordon T 2000
J. Chem. Phys. **113** 9149
[49] Matsumoto M, Saito S and Ohmine I 2002 *Nature* **416** 6879
[50] Baez L A and Clancy P 1995 *J. Chem. Phys.* **103** 9744
[51] Lee C Y, McCammon J A and Rossky P J 1984 *J. Chem. Phys.*
80 4448
[52] Hansen J P and McDonald I R 1996 *Theory of Simple Liquids*
(London: Academic)

[53] Lee S H and Rossky P J 1994 *J. Chem. Phys.* **100** 3334
[54] Berendsen H J C, Postma J P M, van Gunsteren W F,
DiNola A and Haak J R 1984 *J. Chem. Phys.* **81** 3684
[55] Starr F W, Nielsen J K and Stanley H E 1999 *Phys. Rev. Lett.*
82 2294
Starr F W, Nielsen J K and Stanley H E 2000 *Phys. Rev.* E
62 579
[56] Gallo P and Rovere M 2003 *J. Phys.: Condens. Matter* **15** 7625
[57] Dokter A M, Woutersen S and Bakker H J 2005 *Phys. Rev. Lett.*
94 178301
Dokter A M, Woutersen S and Bakker H J 2006 *Proc. Natl
Acad. Sci. USA* **103** 15355
[58] Balasubramanian S, Pal S and Bagchi B 2002 *Phys. Rev. Lett.*
89 115505
[59] Paul S and Chandra A 2004 *Chem. Phys. Lett.* **386** 218
[60] Hummer G, Rasaiah J C and Noworyta J P 2001 *Nature*
414 188
[61] Hanasaki I and Nakatani A 2006 *J. Chem. Phys.* **124** 174714
[62] Luzar A and Chandler D 1993 *J. Chem. Phys.* **98** 8160
Luzar A and Chandler D 1996 *Nature* **379** 55
Luzar A and Chandler D 1996 *Phys. Rev. Lett.* **76** 928
[63] Chu X-Q, Kolesnikov A I, Moravsky A P, Garcia-Sakai V and
Chen S-H 2007 *Phys. Rev.* E **76** 021505
[64] Martí J, Pardro J A and Guàrdia E 1996 *J. Chem. Phys.*
105 639
[65] Montrose C J, Bucaro J A, Marshall-Coakley J and
Litovitz T A 1974 *J. Chem. Phys.* **60** 5025
Danninger W and Zundel G 1981 *J. Chem. Phys.* **74** 2769
Conde O and Teixeira J 1984 *Mol. Phys.* **53** 951